Methodology for Water monitoring in the Upper Troposphere with Raman Lidar at Observatory of Haute-Provence

Christophe Hoareau[1], Philippe Keckhut[1], Alain Sarkissian[1], Jean-Luc Baray[2], Georges Durry[3]

[1]LATMOS, Reduit de Verrieres – BP3, Route des Gatines, 91371 Verrieres-le-Buisson Cedex (France),
[2]LACy, 15 avenue Rene Cassin – BP 7151, 97715 Saint-Denis Messageries Cedex 09 (France),
[3]GSMA, Moulin de la Housse – BP 1039, 51687 Reims Cedex 2 (France),

ABSTRACT

A Raman water vapour lidar has been developed at Observatory of Haute-Provence to study the distribution of water in the upper troposphere and its long term evolution. Some investigations have been proposed and described to ensure a pertinent monitoring of water vapour in the upper troposphere. A new method to take into account the geophysical variability for time integration processes has been developed based on the stationary of water vapour. Successive measurements, considered as independent, have been used to retrieve H_2O profiles that were recorded during the same nighttimes over a few hours. Various calibration methods including zenith clear sky observation, standard meteorological radiosondes and total water vapour column have been investigated. A method to evaluate these calibration techniques has been proposed based on the variance weakening. For the lidar at the Observatory of Haute-Provence, the calibration based on the total water vapour column appears as the optimum method. Radiosondes give also comparable results but do not allow lidar being independent. The clear sky zenith observation is an original technique and seems to accurately identify discontinuities. However it appears to be less reliable based on the variance investigation than the two others. It is also sensitive to aerosol loading which is also expected to vary with time.

INTRODUCTION

Water vapour is a key atmospheric constituent in the global radiation budget, and plays a main role because of its efficiency as a greenhouse gas. Despite its distribution in the atmosphere and its importance for the climate system, many questions regarding H_2O are presently unresolved [1]; including the stratospheric water vapour trends. In the stratosphere water vapour has increased of 2 ppmv since the 1950's which is not negligible compared to the mean values observed in this region (4-6 ppmv)[2]. Water vapour distribution in the upper troposphere (UT) and lower stratosphere (LS) is not perfectly understood due to the numerous processes involved, the high spatiotemporal variability, the phase changes and the transport processes. It is then essential to improve our knowledge about water vapour in this region of the atmosphere with adequate resolutions.

Given the difficulties to measure accurately water vapour in UTLS, a large number of techniques have been developed (microwaves, GPS, specific sondes, radar, lidar...). Many of them cannot provide long-term monitoring of water vapour [3]. Lidar instrument allows probing continuously water vapour with a good sensitivity and vertical resolution. Raman lidar presents the advantage to be implemented in existing backscattering lidar, and since the work of Cooney et al. [4] a larger community of researchers has been using such additional channels [5, 6, 7, 8]. However the calibration issues are still pending: indeed, a proper calibration is necessary to provide an absolute measurement of water vapour mixing ratio. The calibration coefficients are commonly determinate from nearby meteorological radiosondes but their reliability for long-term continuity is questionable [9] and independent techniques will be preferred. Other methods need also to be evaluated [10, 11], including the one proposed by Sherlock et al. [10] based on daytime zenith sky observations.

Because Raman signals are small compared to elastic backscattered ones, long integration times are required to cover accurately the upper troposphere. Averaging processes reduce the variability scale but also mix several situations that may not exist simultaneously. That is a problem for water vapour climatology investigations. Nevertheless, the possibility to acquire elastic signal simultaneously with water vapour Raman signals is a great interest for the sounding the upper troposphere while it provides information about ice crystal occurrence.

LIDAR DESCRIPTION AND ANALYSIS

1.1 Description of the Lidar implanted at Observatory of Haute-Provence

Raman lidar water vapour implemented at Observatory of Haute-Provence (43.9°N, 5.7°E, elevation 685m) is in fact an upgrading of the receiving optics of the existing Rayleigh temperature lidar that is part of the NDACC (Network for the Detection of Atmospheric Composition Change), and operates on a routine basis at night, except in the presence of low cloud [6]. A Nd:YAG laser pulse at 532.1 nm is emitted vertically through the atmosphere at a rate of 50 Hz. The backscattered signals are collected by optical fibers mounted in the focal plane of a 4-telescopes mosaic of 0.5-m-diameter each and transferred to the optical ensemble. A small field of view of 0.5 mrad is used to reduce at maximum the sky background, even if the measurements are essentially performed at nighttimes. The parallax design (emission-reception axis of 0.6 m) of this lidar exhibits a dead altitude zone from the ground up to 2-3 kilometers as a consequence of the small field of view. The Raman shifted lines H_2O (660 nm) and N_2 (607 nm) are separated with a dichroic mirror and are detected by means of photomultiplier tubes (PMT) operated in photo-counting mode. Counts from 8000 shots (~2 min 40 s) are pre-accumulated in 75-m (0.5 µs) bin intervals and stored to constitute the raw data.

© Proceedings of the 8th International Symposium on Tropospheric Profiling, ISBN 978-90-6960-233-2
Delft, The Netherlands, October 2009. Editors, A. Apituley, H.W.J. Russchenberg, W.A.A. Monna

1.2 Measurement Errors Analysis

Because systematic errors have been reduced by hardware design, the signal processing relating to the measurements uncertainties is based on random errors [6]. The two principal error sources considered here are photon-counting and skylight background estimation. The photon-counting process is described by Poisson statistics and the standard deviation of the measurement is $\sigma=\sqrt{N}$ where N is the number of photons counted. The skylight background noise, b_x, is due to skylight brightness, thermal noise of the multiplier and signal induce noise due to large initial burst. The background noise signal is approximated by a least square fitting method. The noise model is an issue for the upper troposphere range (altitude 75 km - 150 km) where signal is small compared to noise.

In order to reduce the statistical noise a temporal and vertical integration has been applied on raw data which permits to extend the altitude range in upper troposphere. The minimum integration time that we have decided to use is ~25 minutes; it is the best compromise to access the variability. The vertical integration is an average window growing with altitude. Thus, in the lower troposphere, as the return signal is large, the initial 75 meters are not degraded. In the middle and upper troposphere, the vertical resolution increases up to 1 km. Random errors increase to 10 % at 6 km and can increase up to 60 % at around 10 km.

1.3 Data Analysis

The water vapor mixing ratio is based on the ratio of the H_2O Raman (660 nm) and the N_2 Raman signal (607 nm) as described by Sherlock et al. [6] accounting the atmospheric differential transmission $\Gamma(z)$ and the calibration coefficient C:

$$q(z) = C.\Gamma(z).\frac{S_{H_2O}(z)}{S_{N_2}(z)}, \qquad (1)$$

In the middle and upper troposphere aerosols densities are generally small and ice clouds do not exhibit large wavelength attenuation dependence. Although it can be estimated with additional channels [12], it has been shown that the relative transmission of the Raman returns corresponds to a 0-5 % overestimation in extreme aerosol loading conditions. Furthermore for altitude above 4 km the vertical gradients of $\Gamma(z)^{-1}$ was small (<0.2 % km^{-1}) and negligible: consequently, no attenuation corrections have been applied [6].

The optical thickness of cirrus is calculated in accordance with the Scattering Ratio profile (SR) which is determinated by the following expression:

$$SR = \frac{\beta_{aerosol}(\lambda,z) + \beta_{rayleigh}(\lambda,z)}{\beta_{rayleigh}(\lambda,z)}, \qquad (2)$$

Where $\beta_{aerosol}(\lambda,z)$ and $\beta_{rayleigh}(\lambda,z)$ are respectively the Mie backscattering and Rayleigh backscattering coefficients. Because molecular backscattering can be estimated by dry air density profile, it can further be retrieved from the nitrogen signal. So *SR* can be derived from the ratio between the return signal at 532 nm and nitrogen Raman signal [13].

The optical thickness of cirrus, ζ_{cirrus}, is calculated in using a method similar to that described by Goldfarb et al. [14] where ζ_{cirrus} can be expressed by the following expression:

$$\tau_{cirrus} = (LR).\sigma_{rayleigh} \int_{Z_{\min}}^{Z_{\max}} n_{air}(z).(SR(z)-1)dz, \qquad (3)$$

Where $\beta_{rayleigh}=\sigma_{rayleigh}.n_{air}(z)$, and $n_{air}(z)$ air density number are calculated by the MSISE-90 atmospheric model. A Lidar Ratio (LR) of 18.2 sr [15] is used, and $\sigma_{rayleigh}(532nm)=5.7x10^{-32}\ m^2\ sr^{-1}$.

DATA SAMPLING

For stationary atmospheric conditions, the photons backscattered hit the counter independently and the counting is a Poisson process. The sampling period must be chosen long enough for collecting a sufficient number of counts (~25 minutes) to provide the best statistical estimator of the water vapor mixing ratio. However, if the sampling period is too long, information about the variability of the local concentration is lost.

In order to get a reasonable compromise between accuracy and atmospheric variability, the proposed method consists of adjusting the integration time with the discontinuity of the flow sounded. To achieve this goal, the series of the ratio of the raw data have been statistically investigated to identify discontinuities at several altitude heights.

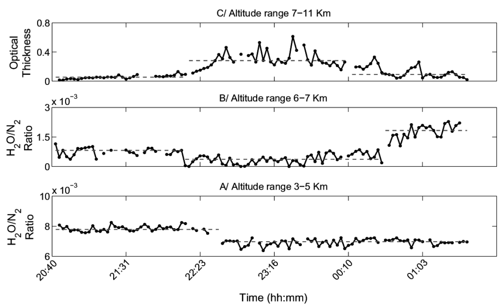

Figure 1. *Evolution of optical thickness in altitude range 7-11 km, and vertically integrated H_2O/N_2 in the altitude range 3-5 km and 6-7 km; within time on the abscissa. One time represent an average of 8000 shots (2'40"). These variations are represented by black solid line and the medians by the grey dashed lines.*

The analysis is conducted on three altitude ranges (3-5 km, 6-7 km and 7-11 km)(Figure 1). For each altitude range and each integrated profile (over 2 min 40 s), the vertically integrated value of water vapor content is performed. Nevertheless this procedure is only done for the altitude range 3-5 km and 6-7 km because at higher altitudes, water vapor density is weak. Because between 7 km and 11 km it is difficult to determine correctly this value and because at higher altitudes the system is limited for H_2O measurement, the analysis of the cirrus optical thickness series in this altitude range is preferred to represent the variability. The identification of discontinuities in the time series is based on the test of non-stationarity of the series due to a change in the dispersion (variance). The procedure applied is an iterative method designed to research the multiple change-points in arbitrary values series [16]. This method is based on the method of the non-parametric test (Wilcoxon-Mann-Whitney distributional test), followed by an adjustment of the median; the process is reiterated until a significant continuity is achieved. Depending of the periods analyzed, 2 to 5 periods can be identified during a complete night. An example is given in figure 2 and 3.

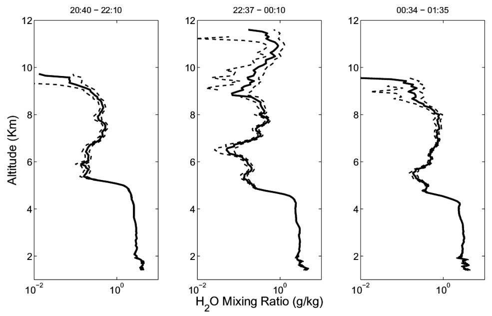

Figure 2. *Vertical profiles of water vapour obtained by lidar during the same night of measurements on May 28th, 1999. The total time of the measurements is 20:40-01:35 UT. The 3 profiles correspond to 3 distinct periods when geophysical changes of large vertical scales have been found significantly unchanged (quasi stationary geophysical conditions) over the three altitude levels (3-5 km, 6-7 km, 7-11 km). The integration times are indicated above each profile. The water vapour mixing ratio is represented in solid line and the errors in dashed line.*

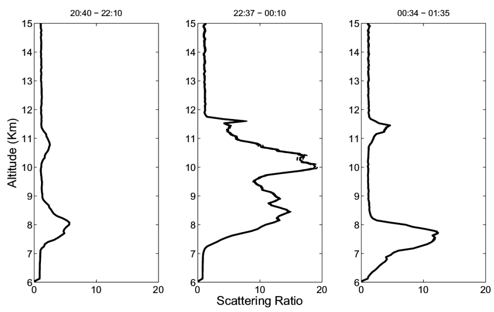

Figure 3. *Vertical profiles of scattering ratio obtained by lidar during the same night of measurements on May 28th, 1999. Same as Figure 2 except for scattering ratio profile. Error bars are very small and not readable in these figures.*

CALIBRATION METHODS

The application of lidar measurement to climatological study requires a robust calibration of the instrument. The evolution of the calibration coefficient over long enough period permits to adjust the series to the instrumental changes which are unavoidable in long commitment (ageing and/or substitution of filters, fiber-optic, receiving optic alignment, detectors...). In this section, three calibration methods are briefly described and have been compared over the period from May 1999 to December 2000.

1.1 Description of calibration methods

One of these methods of calibration used here is based on the systematic observation of the sky with the lidar having the laser off and the neutral density filter on which was developed by Sherlock et al. [10]. The ratio of the two Raman channels during daytime provides useful information about the nighttime calibration coefficient. This method assumes that calibration coefficient is stable and mainly due to instrumental changes and that the daytime measurements are correlated with nighttime laser observations.

The calibration method using collocated radiosonde measurements does not appear as an optimal method and is questionable for independent long-term lidar monitoring given the numerous problems of discontinuity on individual station and the poor sensitivity in upper troposphere. However, it is valuable to compare this approach with other methods. Due to the very high spatial and temporal variability of water vapour, calibration studies are more appropriate if the measurements are effected simultaneously and from the same location. In this analysis, we have considered the radiosondes of Nîmes (distance to OHP < 100 km) for the calibration. The raw lidar signals are integrated over a time period of a least 25 minutes close to the radiosonde measurement times and taking into account the variability following the procedure described in the previous section.

The calibration method with total column measurements is possible if the lidar profiles cover the altitude range where water vapour is distributed. The water vapour content is located at ~99% in the troposphere. As the lidar profile is optimized for the upper troposphere, there is no measurement below 2-3 km. Because balloon measurements are quite reliable in the lower troposphere, the lidar profile is extended downward in using the radiosondes after being used to normalize lidar profiles. Above the top of the lidar profile, an extension upward is made based on a climatology that used HALOE and MLS data, because this additional water vapour contribution is quite small. Here the water vapour total column is obtained from the Elodie spectra. Elodie is a high resolution visible spectrometer mounted on the 1.93 m telescope of the Observatory of Haute-Provence and which has operated between 1995 and 2005 [17]. Water vapor is measured at 593 nm by absolute optical absorption spectrometry [18].

1.2 Comparison of the calibration methods

To perform a more quantitative estimate of the calibration coefficients, the lidar water vapour mixing ratio calibrated with 3 methods, in the altitude range 2-7 km has been calculated. The signals observed result of the contribution of geophysical variability with various superimposed errors associated to the instrument (optical fiber transmission, filter efficiency...) and data processing (noise extraction, calibration...). Both contributions being independent, we define the observed variance as the sum of the geophysical variance and the variance of error. Because the number of profiles is reasonably large, thus a decrease of the observed variance of the mixing ratio series calibrated by one or another method could inform about the reduction of the instrumental discontinuities calibrated series.

The investigation of the calibration methods based on the variance weakening has shown that the method using zenith clear sky observations did not provide as good results as the calibration from radiosonde which permits to improve the calibration reducing the observed variance of 10% at all height. However zenith clear sky observations method seems to be better for the detection of instrumental changes. The results obtained according to these methods suggest that the hypothesis that the system behaves similarly during nighttime and daytime is not valid. The both calibration methods are in agreement with the instrumental changes, however clear sky calibration method gives the best results in detecting discontinuities because is more sensible and so identifies more clearly jumps of the calibration coefficient. The illumination conditions of the photomultipliers are different according to daytime sky background calibration that is based on the filter shape or nighttime laser operations that is related to beam transmission. Also the better results for the calibration have been obtained from the method using total column which tends to improve the radiosonde method. Even if the fact to extend the lidar profile downward from radiosonde in order to use total column is not an optimal solution, the method seems to be a good compromise in the improvement of the calibration.

REFERENCES

[1] Bates B. C., Z. W. Kundzewicz, S. Wu and J. P. Palutikof, Eds., 2008: Climate Change and Water Technical Paper of the Intergovernmental Panel on Climate Change, IPCC Secretariat, Geneva, 210 pp.

[2] Kley D. J. M., Russell III, and C. Philips (Eds.): SPARC assessment of upper tropospheric and stratospheric water vapour, WCRP 113, WMO/TD No. 1043, SPARC Report No. 2, 312 pp., 2000

[3] Durry G., and I. Pouchet, 2001: A Near-Infrared Diode Laser Spectrometer for the In Situ Measurement of Methane and Water Vapor from Stratospheric Balloons, *J. Atmos. Ocean. Technol.*, **18**, pp. 1485-1494

[4] Cooney, J., 1970: Remote measurement of atmospheric water vapor prolifes using Raman component of laser backscatter, *J. Appl. Meteorol.*, **9**, pp. 182-184.

[5] Sherlock V. J., A. Garnier, A. Hauchecorne, and P. Keckhut, 1999: Implementation and validation of a Raman backscatter lidar measurement of mid and upper tropospheric water vapour, *Appl. Opt.*, **38**, pp. 5838-5850

[6] Leblanc. T., I. S. McDermid, and R. Raspey, 2008: First year operation of a new water vapor Raman Lidar at the JPL-Table Mountain Facility, California, *J. Atmos. Ocean. Technol.*, **25**, pp. 1454-1462

[7] Ferrare R. A., S. H. Melfi, D. N. Whiteman, K. D. Evans, F. J. Schmidlin, and D. O'C. Starr, 1995: A Comparison of Water Vapor Measurements Made by Raman Lidar and Radiosondes, *J. Atmos. Ocean. Technol.*, **12**, pp. 1177-1195

[8] Sakai T., T. Nagai, and M. Nakazato, 2007: Comparisons of Raman Lidar Measurements of Tropospheric Water Vapor Profiles with Radiosondes, Hygrometers on the Meteorological Observation Tower, and GPS at Tsukuba, Japon, *J. Atmos. Ocean. Technol.*, **24**, pp. 1407-1423

[9] Soden B. J., and J. R. Lanzante, 1996: An assessment of satellite and radiosonde climatologies of upper-tropospheric water vapor, *J. Climate*, **9**, pp. 1235-1250

[10] Sherlock V. J., A. Hauchecorne, and J. Lenoble, 1999: Methodology for the independent calibration of Raman backscatter water vapour lidar systems, A*ppl. Opt.*, **38**, pp. 5816-5837

[11] Leblanc T., and I. S. McDermid, 2008: Accuracy of Raman lidar water vapor calibration and its applicability to long-term measurements, *Appl. Opt.*, **47**, pp. 5592-5602

[12] Faduilhe D., P. Keckhut, H. Bencherif, L. Robert, and S. Baldy, 2005: Stratospheric Temperature Monitoring using a vibrational Raman Lidar, Part. 1: Aerosols and Ozone interferences, *J. Environ. Monit.*, **7**, pp. 357-364

[13] Ferrare R. A., D. D. Turner, L. Heilman Brasseur, W. F. Feltz, O. Dubovick, and T. P. Tooman, 2001: Raman Lidar measurements of the aerosol extinction-to-backscatter ratio over the Southern Great Plains, *J. of Geophys. Res.*, **106**, pp. 20333-20347

[14] Goldfarb L., P. Keckhut, M.-L. Chanin, and A. Hauchecorne, 2001: Cirrus climatological results from lidar measurements at OHP (44°N, 6°E), *Geophys. Res. Lett.*, **28**, pp. 1687-1690

[15] Platt C. M. R., and A. C. Dilley, 1984: Determination of the cirrus particle single-scattering phase function from lidar and solar radiometric data, *Appl. Opt.*, **23**, pp. 380-386

[16] Lanzante J. R., 1996: Resistant, Robust and non-parametric techniques for the analysis of climate data: theory and examples, including applications to historical radiosonde station data, *International Journal of Climatology*, **16**, pp. 1197-1226

[17] Moultaka J., S. A. Ilovaisky, P. Prugniel, and C. Soubiran, 2004: The ELODIE Archive, *Publications of the Astronomical Society of the Pacific*, **116**, pp. 693-698

[18] Sarkissian A., and J. Slusser, 2009: Water Vapor Column Measurements using the Elodie Archive at Observatoire of Haute-Provence from 1994 to 2004, *Atmos. Meas. Tech.*, **2**, 319-326